Noise characterization of a pulse train generated by actively mode-locked lasers

Danny Eliyahu, Randal A. Salvatore, and Amnon Yariv

California Institute of Technology, Mail Stop 128-95, Pasadena, California 91125

Received June 22, 1995; revised manuscript received October 25, 1995

We analyze the entire power spectrum of pulse trains generated by a continuously operating actively mode-locked laser in the presence of noise. We consider the effect of amplitude, pulse-shape, and timing-jitter fluctuations that are characterized by stationary processes. Effects of correlations between different parameters of these fluctuations are studied also. The nonstationary timing-jitter fluctuations of passively mode-locked lasers and their influence on the power spectrum is discussed as well. © 1996 Optical Society of America

1. INTRODUCTION

In the past decade a wide variety of continuous-wave mode-locked lasers have been used as reliable sources for ultrashort-pulse measurements. They have been applied in time-resolved spectroscopy, electro-optic sampling, and time-division multiplexing. In these systems the random changes of the imperfectly mode-locked pulse-train properties must be taken into consideration. These random fluctuations are due to fundamental noise sources, such as spontaneous emission, in addition to technical noise sources, such as cavity-length fluctuations.

Autocorrelation measurements are insufficient for the characterization of noise in mode-locked lasers. For this reason the random fluctuations of femtosecond pulse trains are investigated by the technique of radio-frequency spectrum analysis. This technique is based on recording the power spectrum of the laser intensity with a fast photodiode and an electronic spectrum analyzer.

A theoretical description for the low frequencies of the power spectrum under the assumption of stationary processes, given by von der Linde,[1] is typically used to measure the timing-jitter and the intensity rms fluctuations.[2–7] The measurements are based on the approximation that the fluctuations manifest themselves as sideband power around multiples of the fundamental-repetition frequency. The timing-jitter noise leads to an increase in sideband power at higher harmonics, which is proportional to the square of the harmonic number, and the amplitude noise is reflected by harmonic number independent sidebands.

In this paper we intend to fully describe the intensity power spectrum of a train of pulses in the presence of correlated components of stationary random noise. First, in Section 2 the model used to calculate the power spectrum is described. Then we outline, in Sections 3 and 4, the effects of amplitude and timing-jitter fluctuations. The difference between passively and actively mode-locked lasers on the statistics of timing-jitter fluctuations and its influence on the power spectrum are described in Section 4. In Section 5 the effects of independent amplitude and timing-jitter stationary noise together are calculated and the additional contribution of their convolution term is found. The effect of correlations between these fluctuations in the power spectrum is calculated in Section 6. Section 7 describes the autocovariance power spectrum. In Section 8 we study the effect of pulse-shape noise. Section 9 compares experimental data with theory. Conclusions are given in Section 10.

2. MODEL

The detected intensity $I_{\Delta T}$ of a train of $2N + 1$ pulses is described in the time domain as

$$I_{\Delta T}(t) = \sum_{n=-N}^{N} f_n(t - T_n), \tag{1}$$

where f_n is the nth pulse-intensity envelope in the train that occurs at time T_n. The time duration of the $2N + 1$ pulse train is ΔT. In Eq. (1) we assume nonoverlapping electric-field envelopes of neighboring pulses in the train. This assumption is justified for short pulses compared with the repetition period.

According to the Wiener–Khintchine theorem, the power spectrum $P_I(\omega)$ is given in terms of the intensity autocorrelation function $G_I(\tau)$:

$$P_I(\omega) = \int_{-\infty}^{\infty} G_I(\tau)\exp(i\omega\tau)\mathrm{d}\tau, \tag{2}$$

where

$$G_I(\tau) = \lim_{\Delta T\to\infty} \frac{1}{\Delta T} \int_{-\Delta T/2}^{\Delta T/2} I_{\Delta T}(t) I_{\Delta T}(t + \tau)\mathrm{d}t. \tag{3}$$

An alternative description of the power spectrum is given in terms of $I_{\Delta T}(\omega)$,[8]

$$P_I(\omega) = \lim_{\Delta T\to\infty} \frac{1}{\Delta T} \langle I_{\Delta T}(\omega) I^*_{\Delta T}(\omega)\rangle, \tag{4}$$

where

$$I_{\Delta T}(\omega) = \int_{-\Delta T/2}^{\Delta T/2} I_{\Delta T}(t)\exp(i\omega t)\mathrm{d}t, \tag{5}$$

$I^*_{\Delta T}(\omega)$ is the complex conjugate of $I_{\Delta T}(\omega)$, and $\langle\ \rangle$ denotes an ensemble average. Here we assume $I_{\Delta T}(t)$ to be an

0740-3224/96/071619-08$10.00

ergodic function, thus making both time and ensemble averages equivalent.

Without any loss of generality we can assume that the individual event $f_n(t)$ occurs over a short time compared with the observation period ΔT, so the integration limits can be taken as $-\infty$ to ∞ instead of $-\Delta T/2$ to $\Delta T/2$. Therefore we may write

$$I_{\Delta T}(\omega) = \sum_{n=-N}^{N} F_n(\omega)\exp(i\omega T_n), \tag{6}$$

where

$$F_n(\omega) = \int_{-\infty}^{\infty} f_n(t)\exp(i\omega t)\mathrm{d}t. \tag{7}$$

In this case the power spectrum of the pulse train is given by

$$P_I(\omega) = \lim_{N\to\infty} \frac{1}{2N+1} \sum_{n,m=-N}^{N} \langle F_n(\omega)F_m^*(\omega) \times \exp[i\omega(T_n - T_m)]\rangle. \tag{8}$$

The importance of this result is the separation between the fluctuation of the timing jitter, which manifests itself in the exponent, to those of the pulse shape and its amplitude. We can easily calculate the power spectrum by knowing the joint-probability-distribution functions of the fluctuating variables.

In previous research[1,3] the power spectrum was calculated in the time domain [Eqs. (2) and (3)] with the assumption of small stationary timing-jitter fluctuations. This approximation is valid only in the low-frequency power spectrum of actively mode-locked lasers. We find that the calculations in the frequency domain are simplified and free from those assumptions; therefore we use this domain in order to calculate the power spectrum.

In the absence of noise, for a periodic sequence of $2N + 1$ identical pulses, $F_n(\omega) = F(\omega)$, equally separated in time ($T_n = nT$), the power spectrum [Eq. (8)] is

$$P_I(\omega) = |F(\omega)|^2 \lim_{N\to\infty} H_N(\omega T), \tag{9}$$

where T is the pulse-repetition period and

$$H_N(\omega T) = \frac{1}{2N+1}\left|\sum_{n=-N}^{N} \exp(i\omega nT)\right|^2 = \frac{1}{2N+1}\left\{\frac{\sin[(2N+1)\omega T/2]}{\sin(\omega T/2)}\right\}^2. \tag{10}$$

In the limit of an infinite number of pulses, H_N will have the form

$$H(\omega T) = \lim_{N\to\infty} H_N(\omega T) = \frac{2\pi}{T}\sum_{n=-\infty}^{\infty} \delta(\omega - 2\pi n/T). \tag{11}$$

The power spectrum of a perfect, noise-free pulse train is described by a series of Dirac δ functions separated with constant spacing $\Delta\omega = 2\pi/T$, shaped by the squared Fourier transform of the pulse-intensity shape $|F(\omega)|^2$.

3. AMPLITUDE FLUCTUATIONS

Amplitude fluctuations in the pulse trains result from random processes in the laser. Potential sources for amplitude noises are spontaneous-emission and gain fluctuations. Typically, the gain fluctuations have a long relaxation time, and the power of spontaneous emission is relatively small. The amplitude fluctuations occur at a rate that is slow relative to the optical pulse envelope. Therefore it is justified to assume that the output of the laser pulse is described by a set of discrete coherent pulses. Assuming that all the pulses are equally separated in time and equally shaped but differ in amplitude, $F_n(\omega) = A_nS(\omega)$, where $A_n = (A + \delta A_n)$, and A is the real average intensity. The amplitude fluctuations, meaning the difference of the nth pulse from the average intensity A, are described by δA_n. δA_n has zero mean ($\langle\delta A_n\rangle = 0$) and an arbitrary probability-distribution function. Also we assume the fluctuations can be modeled as stationary processes:

$$\langle\delta A_n\delta A_m\rangle = \langle\delta A_0\delta A_{|n-m|}\rangle \tag{12}$$

for a continuously operating mode-locked laser. With Eqs. (8) and (12) the power spectrum is given by

$$P_I(\omega) = |S(\omega)|^2[H(\omega T) + 2P_A(\omega T)], \tag{13}$$

where the Fourier series of $P_A(\omega T)$ is found in terms of the autocorrelations $G_A(k)$ of the amplitude fluctuation occurring at different times:

$$P_A(\omega) = \frac{G_A(0)}{2} + \sum_{k=1}^{\infty} G_A(k)\cos(k\omega T), \tag{14}$$

$$G_A(k) = \langle\delta A_0\delta A_k\rangle. \tag{15}$$

The effect of amplitude fluctuations is to add a periodic spectral density around the Dirac δ functions' discrete lines, i.e., the harmonic-number-independent side-bands. The power added to the power-spectrum continuum reflects the increase of the intensity square that is due to amplitude noise.

4. TIMING-JITTER FLUCTUATIONS

Different sources of noise contribute to fluctuations in the pulse-train timing jitter. Some of these sources are gain, cavity length, refractive index, and spontaneous-emission fluctuations. In this section we concentrate on how these fluctuations are reflected in the power spectrum.

In the case in which there are equally shaped pulses with the same amplitude and random variations of the time interval between successive pulses in the train, i.e., $F_n(\omega) = F(\omega)$ and $T_n = nT + \delta T_n$, the power spectrum is

$$P_I(\omega) = |F(\omega)|^2 \lim_{N\to\infty} \frac{1}{2N+1} \sum_{n,m=-N}^{N} \exp[i\omega T(n-m)] \times \langle\exp[i\omega(\delta T_n - \delta T_m)]\rangle, \tag{16}$$

where T represents the average pulse-repetition period and δT_n describes its fluctuations relative to the time nT of the nth pulse in the train.

In contrast to the amplitude fluctuations, in which the power spectrum depends on the amplitude autocorrelation, in this case, the shape of the power spectrum depends on the full statistics of the timing-jitter fluctuations since it appears in the exponent.

Different types of processes govern the timing-jitter fluctuations for different mode-locked systems. In actively mode-locked lasers, owing to the external restoring force[9] of the active modulation, the timing fluctuations are described by a stationary process.

Assuming stationary processes and a Gaussian probability-distribution function of these fluctuations,

$$\langle \exp[i\omega(\delta T_n - \delta T_m)]\rangle = \exp\{-\omega^2[G_T(0) - G_T(|n-m|)]\}, \tag{17}$$

where $G_T(k)$ is the timing-jitter fluctuation autocorrelation function:

$$G_T(k) = \langle \delta T_0 \delta T_k \rangle. \tag{18}$$

Therefore Eq. (16) has the form

$$P_I(\omega) = |F(\omega)|^2\left[1 + \exp[-\omega^2 G_T(0)]\left(2\sum_{k=1}^{\infty}\{\exp[\omega^2 G_T(k)] - 1\}\cos(k\omega T) + H(\omega T) - 1\right)\right]. \tag{19}$$

The assumption of stationary processes of the pulse-train noise, such as amplitude and timing-jitter fluctuations, are justified since the laser is driven by a stable external timing source. Therefore fluctuations are related to the modulator signal.

The timing-jitter fluctuations result in power-spectrum sidebands. These sidebands differ as a function of harmonic number. Their power comes at the expense of the discrete Dirac δ functions, corresponding to the noiseless laser. The discrete lines are attenuated by a factor $\exp[-\omega^2 G_T(0)]$ that rolls off at high frequencies.

The discrete lines, appearing in the multiplication of the fundamental-repetition frequency, are a direct result of the stationary assumption for the timing-jitter fluctuations that stem from the presence of an external restoring force for active modelocking. In this case the average timing fluctuations $\langle(\delta T_n - \delta T_m)^2\rangle$ are finite for any n, m. This leads to summation of infinite terms over $\cos(k\omega T)$, yielding the discrete δ functions. We prefer to represent the power spectrum as in Eq. (19), since the argument of the sum decays to zero for large k, and the timing-jitter correlation between pulses decreases.

For low frequency $[\omega^2 G_T(0) \ll 1]$ the power spectrum is given as

$$P_I(\omega) = |F(\omega)|^2\{[1 - \omega^2 G_T(0)]H(\omega T) + 2\omega^2 P_T(\omega)\}, \tag{20}$$

where

$$P_T(\omega) = \frac{G_T(0)}{2} + \sum_{k=1}^{\infty} G_T(k)\cos(k\omega T). \tag{21}$$

Equation (19) was calculated with the assumption of a Gaussian probability-distribution function of the timing-jitter fluctuations δT_n. The exact form of the probability is important for the high-frequency power spectrum [see Eq. (16)]. However, the low-frequency power spectra depend only on the second moment $[\langle(\delta T_n - \delta T_m)^2\rangle]$, and the exact form of the probability is unimportant. Therefore Eq. (20) is a general result for stationary processes and is independent of the full probability-distribution function of δT_n. We find the approximation of low frequency to be valid (0.5% relative error) up to $\omega^2 G_T(0) \approx 0.1$, i.e., a harmonic number lower than $n < 0.05T/\sqrt{G_T(0)}$.

In Fig. 1 a plot of $P_I(\omega)/|F(\omega)|^2$ is shown for white noise, i.e., $G_T(k) = G_T(0)\delta_{0,k}$ (where $\delta_{n,m} = 1$ if $n = m$ and zero otherwise). In this case we chose $G_T(0)/T^2 = 10^{-4}$. The sum does not contribute to the power spectrum. The exchanged power grows as the harmonic number increases. This becomes a constant for high frequencies when the power under the discrete lines becomes constant and frequency independent.

In order to see the effect of nonvanishing timing-jitter autocorrelations, we chose $G_T(k) = G_T(0)\exp(-\alpha k)$ as was suggested by Haus *et al.*[9] Figure 2 describes the power spectrum for this autocorrelation, where $\alpha = 1.5$ and $G_T(0)/T_2 = 10^{-4}$. We omitted the factor $\exp[-\omega^2 G_T(0)]H(\omega T)$, which has the effect of attenuating the discrete lines, as shown in Fig. 1. The effect of correlations in timing-jitter fluctuations causes a sharpening of the sidebands. The dashed curve represents the low-frequency approximation, as in Eq. (20), for the maximum peak value; i.e., $2\omega^2 P_T(2\pi/T)$. Approximately five sidebands are in the limit of the low-frequency approximation.

A calculation involving long-range pulse-to-pulse timing-jitter correlations, for $\alpha = 0.5$, is shown in Fig. 3(a). The other parameters are as in Fig. 2. Figure 3(b) shows the first 20 sidebands of the power spectrum as a function of the frequency deviation $\Delta\omega = \omega - 2\pi n/T$ (offset frequency), where n is chosen such that $0 < \Delta\omega < 2\pi/T$. The lower harmonic sidebands do not intersect since, as the harmonic number n increases, the sideband's peak value increases, and its FWHM is approximately constant [see Eq. (20)].

Although in active modelocking an externally applied modulation produces the locking between the longitudinal modes, such external modulation is not needed in passive

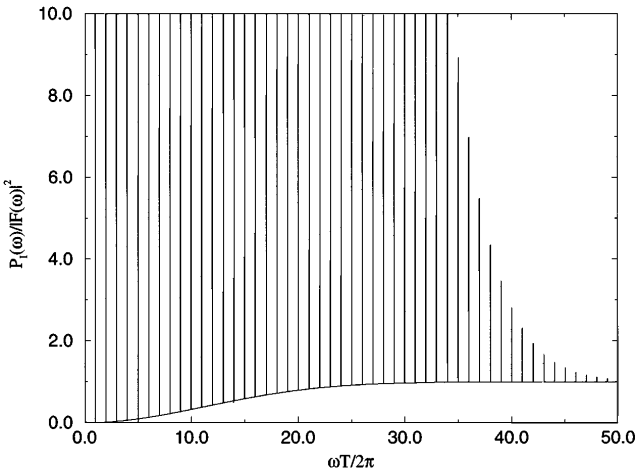

Fig. 1. $P_I(\omega)/|F(\omega)|^2$ as a function of $\omega T/2\pi$ for the stationary white-noise timing-jitter case. Here $G_T(k) = G_T(0)\delta_{0,k}$ and $G_T(0)/T^2 = 10^{-4}$.

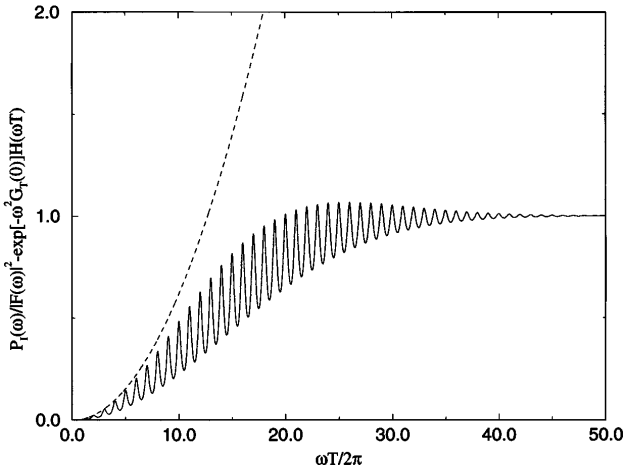

Fig. 2. $P_I(\omega)/|F(\omega)|^2 - \exp[-\omega^2 G_T(0)]H(\omega T)$ versus $\omega T/2\pi$, where $G_T(k) = G_T(0)\exp(-\alpha k)$ and $\alpha = 1.5$. The dashed curve represents the peak values of the power spectrum for low-frequency approximation $[\omega^2 P_T(2\pi/T)]$.

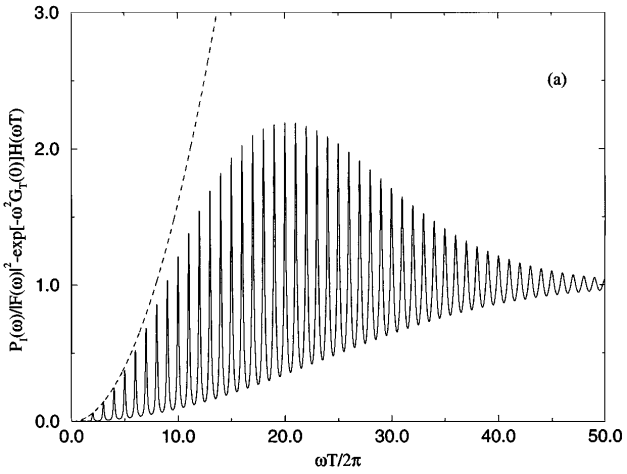

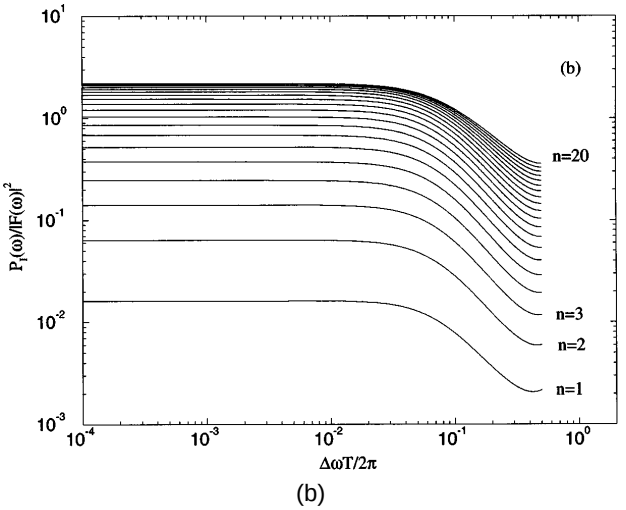

Fig. 3. (a) Same as in Fig. 2, but $\alpha = 0.5$; (b) the power-spectrum sidebands for the first 20 harmonics as a function of the frequency deviation $\Delta\omega$.

mode locking. Instead, the modulation is produced internally and self-consistently through the action of the optical pulse train on the gain and the absorber media. Therefore in passively mode-locked lasers the timing-jitter fluctuations do not obey a stationary process.[9,10] In the absence of a restoring external force the timing of each pulse depends on that of the previous one, and its fluctuation results from the sum of many assumed independent processes. In this case the timing-jitter noise can be described by the random walk or the diffusion theories for Gaussian processes whenever fluctuations of timing jitter between successive neighboring pulses are uncorrelated or when the correlation time is much smaller than the repetition period. The averaged term in Eq. (16) can be written as

$$\langle \exp[i\omega(\delta T_n - \delta T_m)]\rangle = \exp\left(-\frac{\omega^2}{2} DT|n-m|\right), \quad (22)$$

where $D = \langle(\delta T_n - \delta T_{n\pm1})^2\rangle/T$ is the diffusion constant, which describes the timing-jitter fluctuations between successive neighboring pulses. Also, Gaussian probability distributions were assumed for the random $(\delta T_n - \delta T_m)$ timing-jitter fluctuations with zero mean value.

With Eqs. (16) and (22), the summation is performed analytically yielding the power spectrum

$$P_I(\omega) = |F(\omega)|^2 \frac{\sinh(\omega^2 DT/2)}{\cosh(\omega^2 DT/2) - \cos(\omega T)}. \quad (23)$$

In this case the discrete lines, which occur in the stationary approximation, are not valid anymore. Instead, for low-frequency $(\omega^2 DT \ll 1)$ and small-frequency deviation $(\Delta\omega \ll 2\pi n/T)$ the power spectrum is given approximately by Lorentzian functions around multiples of the fundamental-repetition frequency.

In Fig. 4 the first ten side-bands of the power spectrum for the nonstationary case are plotted. These sidebands are given as a function of the frequency deviation $\Delta\omega = \omega - 2\pi n/T$ for $D/2T = 10^{-4}$. As the harmonic number n increases, the peak power decreases and its FWHM increases. Therefore the sidebands intersect. The intersection point between the nth and the mth sidebands for low harmonics numbers $(\omega^2 DT \ll 1)$ are

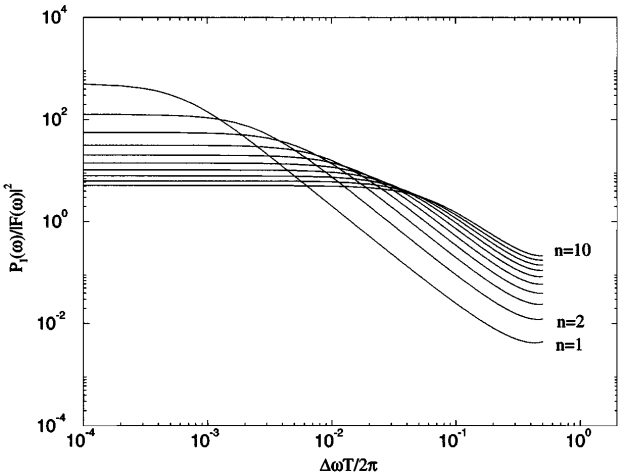

Fig. 4. Power spectrum for the nonstationary timing-jitter fluctuations [Eq. (23)]. The first ten sidebands are plotted as a function of the frequency deviation $\Delta\omega$ in a log-log scale. The value of $D/2T = 10^{-4}$ was assumed.

given by $\Delta\omega_{nm}T/2\pi = \pi Dnm/T$. This characteristic is totally different from that of the stationary timing-jitter fluctuations [see Fig. 3(b)].

In the remainder of this paper we assume the stationary case for the timing-jitter fluctuations, suitable for the actively mode-locked lasers. The nonstationary timing fluctuations, as in the passively mode-locked lasers, are discussed in Ref. 10.

5. STATISTICALLY INDEPENDENT AMPLITUDE AND TIMING-JITTER FLUCTUATIONS

Assuming constant pulse shape in which independent amplitude and timing-jitter fluctuations are present, the average in Eq. (8) can be written as

$$\begin{aligned}\langle F_n(\omega)F_m^*(\omega)\exp[i\omega(T_n - T_m)]\rangle &= |S(\omega)|^2 \exp[i\omega T(n-m)] \\ &\times \langle (A + \delta A_n)(A + \delta A_m)\rangle \\ &\times \langle \exp[i\omega(\delta T_n - \delta T_m)]\rangle . \end{aligned} \tag{24}$$

The power spectrum is given by

$$\begin{aligned} P_I(\omega)/|S(\omega)|^2 &= A^2 + A^2 \exp[-\omega^2 G_T(0)] \\ &\times \left(2\sum_{k=1}^{\infty}\{\exp[\omega^2 G_T(k)] - 1\} \right. \\ &\left. \times \cos(k\omega T) + H(\omega T) - 1\right) \\ &+ G_A(0) + \exp[-\omega^2 G_T(0)] \\ &\times \left\{2\sum_{k=1}^{\infty} G_A(k)\exp[\omega^2 G_T(k)]\cos(k\omega T)\right\} . \end{aligned} \tag{25}$$

In Eq. (25), as before, we assume stationary processes for the amplitude fluctuations and stationary noise with a Gaussian probability-distribution function for the timing jitter, justified in the case of external restoring force.

For low frequency we can evaluate the power spectrum by expanding $\exp[i\omega(\delta T_n - \delta T_m)]$ in a Taylor series, collecting terms up to ω^2, and averaging:

$$\begin{aligned} P_I(\omega) = 2|S(\omega)|^2\{&[1 - \omega^2 G_T(0)][A^2 H(\omega T)/2 + P_A(\omega)] \\ &+ A^2\omega^2 P_T(\omega) + \omega^2 P_A(\omega) \otimes P_T(\omega)\} , \end{aligned} \tag{26}$$

where the convolution of the Fourier series between the amplitude spectrum $P_A(\omega)$ and the timing-jitter spectrum $P_T(\omega)$ is given by

$$\begin{aligned} P_A(\omega) \otimes P_T(\omega) &= \frac{T}{\pi}\int_{-\pi/T}^{\pi/T} P_A(\omega')P_T(\omega - \omega')\mathrm{d}\omega' \\ &= \frac{G_A(0)G_T(0)}{2} + \sum_{k=1}^{\infty} G_A(k)G_T(k)\cos(k\omega T) . \end{aligned} \tag{27}$$

We find a term additional to those considered previously.[1] This extra term is important whenever the pulse train is characterized by relatively high amplitude noise compared with its average value. In this case, in contrast to the calculation of Eq. (25), no assumptions of the specific statistics of the random variables δA_n and δT_n are made. The only approximation is of stationary processes.

6. EFFECT OF DEPENDENT AMPLITUDE AND TIMING-JITTER FLUCTUATIONS

The case of amplitude and timing-jitter fluctuations exhibiting statistical dependence on each other is given in terms of the average

$$\langle (A + \delta A_n)(A + \delta A_m)\exp[i\omega(\delta T_n - \delta T_m)]\rangle . \tag{28}$$

This average is not separable owing to the correlations. The contribution of the lowest-order noise, owing to correlations, is found by expansion of the exponent of Eq. (28) into a series. The terms, including up to the second order in the amplitude and the timing-jitter fluctuations,

$$i\omega A\langle(\delta A_n + \delta A_m)(\delta T_n - \delta T_m)\rangle = 0 , \tag{29}$$

vanish owing to symmetry for stationary processes. This result is reasonable since the power spectrum of a real signal is real, positive, and an even function of ω. Therefore we expect the contribution from this statistical dependence to be in a higher order than those of the amplitude $G_A(k)$ or timing jitter $G_T(k)$. This result is important, since it shows that the correlations contribute in a smaller order of magnitude, which for relatively small fluctuations may be negligible.

The average in Eq. (28) is easily found by assuming stationary processes with Gaussian probability-distribution functions for both the amplitude and the timing jitter:

$$\begin{aligned} &\langle (A + \delta A_n)(A + \delta A_m)\exp[i\omega(\delta T_n - \delta T_m)]\rangle = \\ &\quad \{A^2 + G_A(|n-m|) + \omega^2[G_{AT}(0) - G_{AT}(|n-m|)]^2\} \\ &\qquad \times \exp\{-\omega^2[G_T(0) - G_T(|n-m|)]\} , \end{aligned} \tag{30}$$

where $G_{AT}(k) = \langle \delta A_0 \delta T_k\rangle$ describes the amplitude to timing-jitter correlations. As expected, the dependence is on $G_{AT}^2(k)$, i.e., higher order in the amplitude and the timing-jitter correlations. In developing Eq. (30) the joint characteristic function nature of the Gaussian probability-distribution function was used.

The power spectrum has the form

$$\begin{aligned} P_I(\omega)/|S(\omega)|^2 &= A^2 + A^2 \exp[-\omega^2 G_T(0)] \\ &\times \left(2\sum_{k=1}^{\infty}\{\exp[\omega^2 G_T(k)] - 1\} \right. \\ &\left. \times \cos(k\omega T) + H(\omega T) - 1\right) \\ &+ G_A(0) + \exp[-\omega^2 G_T(0)] \\ &\times \left(2\sum_{k=1}^{\infty}\{G_A(k) + \omega^2[G_{AT}(0) - G_{AT}(k)]^2\} \right. \\ &\left. \times \exp[\omega^2 G_T(k)]\cos(k\omega T)\right) . \end{aligned} \tag{31}$$

The constant term, $G_{AT}(0)$, in the sum contributes to the discrete lines (see Section 7). The component of the power spectrum that results from this term has the form

$$\begin{aligned} \omega^2 \exp[-\omega^2 G_T(0)][G_{AT}(0)]^2 &\left(2\sum_{k=1}^{\infty}\{\exp[\omega^2 G_T(k)] - 1\} \right. \\ &\left. \times \cos(k\omega T) + H(\omega T) - 1\right) . \end{aligned} \tag{32}$$

For non-Gaussian statistics, terms of different order in δA_n, δT_n (for example, $A\omega^2\langle\delta A_n\delta T_n\delta T_m\rangle$) can contribute to the power spectrum. Still, this contribution is less than $G_A(k)$ or $A^2\omega^2G_T(k)$ for relatively small fluctuations. Therefore amplitude to timing-jitter correlations contribute to the low-frequency power spectrum in the same fashion as the convolution between themselves, i.e., including ω^2 terms multiplied by $\langle\delta A_0\delta A_k\rangle\langle\delta T_0\delta T_k\rangle$ in the convolution terms and $\langle\delta A_0\delta T_k\rangle^2$ in the correlation terms. In both cases these are proportional to a multiplication by the squared amplitude fluctuations and the squared timing-jitter fluctuations.

Assuming that $|S(\omega)|^2$, $\exp[-\omega^2G_T(k)]$ and $\exp[\omega^2G_T(k)]$ do not vary strongly in the range $2\pi(n-1/2)/T$ to $2\pi(n+1/2)/T$, around the nth harmonic number, the integration over this range of the power spectrum in Eq. (31),

$$\frac{1}{|S(2\pi n/T)|^2}\frac{T}{2\pi}\int_{2\pi(n-1/2)/T}^{2\pi(n+1/2)/T}P_I(\omega)\mathrm{d}\omega = A^2 + G_A(0), \tag{33}$$

is independent of n. The parts of the discrete lines that are not due to the correlations [see Eq. (32)] cancel the contribution of $P_T(\omega)$. The contributions of the convolution and the correlation terms also vanish and do not contribute to this integral.

In order to measure the rms fluctuations, one can evaluate the integral in different regimes. For low frequency $[\omega^2G_T(0) \ll 1]$ and assuming relatively small fluctuations, we can approximate

$$\frac{T}{\pi}\int_{\omega_L}^{\omega_H}P_I(\omega)\mathrm{d}\omega \simeq G_A(0) + \left(\frac{2\pi n}{T}\right)^2[A^2G_T(0) - G_{AT}^2(0)], \tag{34}$$

where $\omega_L \to 2\pi n/T$ and $\omega_H = 2\pi(n+1/2)/T$. In this way, by choosing correctly ω_L, we can eliminate the contribution of the Dirac δ function to the integral. Also, it is assumed that $|S(\omega)|^2$ does not vary for low frequency and was chosen as a unit constant. The assumption $G_{AT}^2(0) \ll A^2G_T(0)$ (justified for relatively small amplitude fluctuations) allows one to approximate the rms amplitude and timing-jitter fluctuations.

In a similar fashion one can measure the amplitude and the timing-jitter autocorrelations. Using the same assumptions as before, we have

$$\begin{aligned} b_n(k) &= \frac{T}{\pi}\int_{\omega_L}^{\omega_H}P_I(\omega)\cos(k\omega T)\mathrm{d}\omega \\ &\simeq G_A(k) + A^2\left(\frac{2\pi n}{T}\right)^2G_T(k). \end{aligned} \tag{35}$$

The normalized autocorrelations are found in terms of $b_n(k)$ as

$$G_T(k)/G_T(0) = \frac{b_n(k) - b_m(k)}{b_n(0) - b_m(0)}, \tag{36}$$

$$G_A(k)/G_A(0) = \frac{m^2b_n(k) - n^2b_m(k)}{m^2b_n(0) - n^2b_m(0)}, \tag{37}$$

where $m \neq n$. This result can be calculated for different pairs of m and n of low harmonic numbers.

7. AUTOCOVARIANCE POWER SPECTRUM

The discrete lines appearing in Eq. (31) and expression (32) for the power spectrum arise from the fact that, in the stationary noise assumption, a nonzero amount of power is concentrated at the particular frequencies $2\pi n/T$. We may avoid the difficulties arising in connection with these Dirac δ functions by forming a new random variable. We obtain this variable by subtracting the averaged signal $[I_{\Delta T}(t) - \langle I_{\Delta T}(t)\rangle]$ and by measuring the autocovariance power spectrum:

$$P_I^C(\omega) = \lim_{\Delta T\to\infty}\frac{1}{\Delta T}\langle I_{\Delta T}(\omega)I_{\Delta T}^*(\omega)\rangle_C, \tag{38}$$

where $\langle AB\rangle_C \equiv \langle AB\rangle - \langle A\rangle\langle B\rangle$.

Assuming stationary processes and Gaussian probability-distribution functions for the amplitude and the timing jitter with a consistent pulse shape, the contribution of the discrete lines is given by

$$\begin{aligned} \lim_{\Delta T\to\infty}\frac{1}{\Delta T}\langle I_{\Delta T}(\omega)\rangle\langle I_{\Delta T}^*(\omega)\rangle &= |S(\omega)|^2\{A^2 + [\omega G_{AT}(0)]^2\} \\ &\times H(\omega T)\exp[-\omega^2G_T(0)]. \end{aligned} \tag{39}$$

Therefore the autocovariance power spectrum $P_I^C(\omega)$ has the same form as $P_I(\omega)$ without the Dirac δ function contributions.

8. AMPLITUDE AND PULSE-SHAPE FLUCTUATIONS

The study of the power spectrum including pulse-shape fluctuations is limited and less general since it depends on the explicit shape of the laser pulses. In this section we give a qualitative description of the power spectrum in the presence of pulse-shape fluctuations. The simplest case of Eq. (8) can be achieved through the assumption of statistically independent pulse-shape parameters describing each pulse in the train. We also assume pulses equally separated in time. In the case of pulses possessing shape and amplitude fluctuations that have no correlations between different pulses, i.e.,

$$\langle F_n(\omega)F_m^*(\omega)\rangle = \begin{cases}\langle|F_n(\omega)|^2\rangle & n = m \\ |\langle F_n(\omega)\rangle|^2 & n \neq m\end{cases}, \tag{40}$$

where fluctuation parameters are averaged, the power spectrum has the form

$$P_I(\omega) = \langle|F_n(\omega)|^2\rangle + |\langle F_n(\omega)\rangle|^2[H(\omega T) - 1]. \tag{41}$$

The term $\langle|F_n(\omega)|^2\rangle - |\langle F_n(\omega)\rangle|^2$ is reflected as sidebands around the delta functions at the harmonics. The remaining terms describe the discrete line's contribution to the power spectrum.

For simplicity we assume Gaussian-shaped pulses with duration and amplitude fluctuations. The less likely case of constant amplitude and Gaussian-shaped pulses with duration fluctuations is analyzed first. The aim of this example is to show that duration fluctuations have effects similar to those of the amplitude on the low-frequency power spectrum.

The pulse shape is given by

$$f_n(t) = \exp\left[-\frac{t^2}{2(\tau + \delta\tau_n)^2} \right], \tag{42}$$

where unity amplitude is assumed. Its Fourier transform gives

$$F_n(\omega) = \sqrt{2\pi}(\tau + \delta\tau_n)\exp\left[-\frac{\omega^2(\tau + \delta\tau_n)^2}{2} \right]. \tag{43}$$

For low frequency the power spectrum has the form

$$P_I(\omega) \simeq \tau^2\left\{1 - \omega^2[\tau^2 + 3G_\tau(0)]\right\} \times H(\omega T) + 2P_\tau(\omega)(1 - 3\tau^2\omega^2), \tag{44}$$

where $P_\tau(\omega) = G_\tau(0)/2 + \sum_{k=1}^{\infty} G_\tau(k)\cos(k\omega T)$ and $G_\tau(k) = \langle \delta\tau_0 \delta\tau_k \rangle$. The calculation was done by expansion of Eq. (43) into a Taylor series in frequency. Although the pulse in the time domain has constant peak amplitude, its duration fluctuations appear on the low-frequency power spectrum sidebands in a form similar to Eq. (13), which describes the result of pulse-amplitude fluctuations. In higher harmonics it decays as ω^2, which can eliminate the contribution of the timing-jitter rms fluctuations.

Equation (44) is in agreement with Fuss,[11] who studied the low-frequency power spectrum of pulses exhibiting the general form of $f_n(t) = (A + \delta A_n)\phi_n[t/(\tau + \delta\tau_n)]$, where $\phi_n(0) = 1$.

The amplitude and the pulse-duration fluctuations would be highly correlated when pulse energies remain constant. Otherwise, one would require systematic energy transfer into and out of the laser modes to change the mode-locked optical spectrum width. The amplitude and the pulse-duration fluctuations can be a result of chirp fluctuations in the frequency domain. The pulse-intensity shape is given by

$$f_n(t) = \frac{1}{\tau + \delta\tau_n} \exp\left[-\frac{t^2}{2(\tau + \delta\tau_n)^2} \right], \tag{45}$$

where τ is the average pulse duration and $\delta\tau$ is the fluctuation in the pulse duration. Since the pulse energy is normalized, a change in the pulse duration causes a change in the pulse amplitude.

In the frequency domain, $F_n(\omega)$ is given by the Fourier transform of Eq. (45):

$$F_n(\omega) = \sqrt{2\pi} \exp\left[-\frac{\omega^2(\tau + \delta\tau_n)^2}{2} \right]. \tag{46}$$

The energy of each pulse is given by $F_n(0)$.

Assuming a Gaussian probability-distribution function with zero mean for $\delta\tau_n$ and averaging the relevant powers of F_n gives

$$|\langle F_n(\omega)\rangle|^2 = \frac{2\pi}{1 + \omega^2 G_\tau(0)} \exp\left[-\frac{\tau^2\omega^2}{1 + \omega^2 G_\tau(0)} \right], \tag{47}$$

$$\langle |F_n(\omega)|^2 \rangle = \frac{2\pi}{\sqrt{1 + 2\omega^2 G_\tau(0)}} \exp\left[-\frac{\tau^2\omega^2}{1 + 2\omega^2 G_\tau(0)} \right], \tag{48}$$

where $G_\tau(0) = \langle \delta\tau_n^2 \rangle$.

The region of interest is the low-frequency power spectrum. In this region the sidebands are described by $\langle |F_n(\omega \to 0)|^2 \rangle - |\langle F_n(\omega \to 0)\rangle|^2$, which, by Eqs. (47) and (48), are found to have small contributions. The power spectrum has the form of

$$P_I(\omega) \simeq 2\pi\omega^4\tau^2 G_\tau^2(0) + 2\pi\{1 - \omega^2[\tau^2 + G_\tau(0)]\}H(\omega T). \tag{49}$$

The low-frequency power spectrum can be easily analyzed for the correlated pulse-to-pulse $\delta\tau_n$ fluctuations in the Gaussian pulse shape. The calculation is made for small ω by expansion of Eq. (46) in a Taylor series in frequency. The power spectrum is found to have a form similar to that for the uncorrelated $\delta\tau_n$ [Eq. (49)]. It introduces terms of ω^4 in the relative height of the harmonic sidebands.

We can conclude that shape fluctuations can eliminate the effect of amplitude fluctuations. This will result in the low-frequency region having small and hard-to-detect sidebands. Sidebands of small harmonic number in the power spectrum are used to measure amplitude rms noise. The joint amplitude and pulse-duration fluctuations are not reflected in these first sidebands although pulses differ from each other.

From these examples we learn that energy fluctuations control the low-frequency power-spectrum sidebands. These fluctuations result from amplitude and shape fluctuations. In the absence of energy fluctuations these sidebands are small, and the power spectrum is characterized by almost perfect discrete lines.

9. EXPERIMENTAL RESULTS

In this section we examine briefly the existing experimental data on timing-jitter and amplitude fluctuations of actively mode-locked lasers. Many experimental results have been published so far on timing jitter of lasers that have been actively modelocked. Generally, it is difficult to obtain, from the published experiments, all the information on the power-spectrum sideband shapes. We additionally analyzed the results obtained by Finch *et al.*[4] for the synchronously mode-locked KCI:Ti color-center laser. In this paper the amplitude and the timing-jitter rms fluctuations were measured. The apparent power spectrum [Fig. 6(a) in Ref. 4] clearly shows a shape similar to the result of Eq. (25) when the effects of pulse shaping and amplifier response are taken into account. The values of the power spectrum, at frequencies equal to $\omega T = 2\pi(n + 1/2)$ (the low values of the power spectrum), increase as the frequency increases.

Since the timing-jitter and the amplitude fluctuations were found to be relatively small (see Table 1 in Ref. 4), the convolution term and the correlation between timing-jitter and amplitude fluctuations are negligible. Therefore using Eqs. (35)–(37) in order to calculate the timing-jitter and the amplitude autocorrelations is justified. These results are plotted in Fig. 5. Figure 5(a) describes the normalized timing-jitter autocorrelation $G_T(k)/G_T(0)$ (solid curve) and the normalized amplitude autocorrelation $G_A(k)/G_A(0)$ (dotted curve) in which the integration boundaries on the power-spectrum sidebands are from 25 Hz to 500 Hz. We performed the calculations for $n = 1$ and $m = 10$ [see Eqs. (36) and (37)] by using

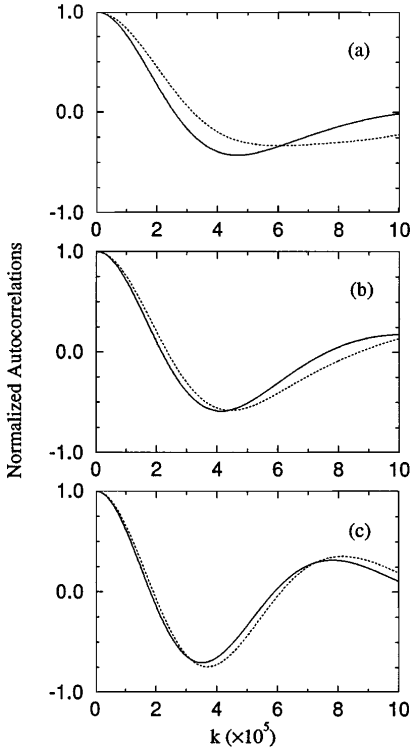

Fig. 5. Normalized timing-jitter autocorrelation $G_T(k)/G_T(0)$ (solid curves) and the normalized amplitude autocorrelation $G_A(k)/G_A(0)$ (dotted curves) as a function of $k = t/T$, the ratio between the measured time to the repetition period. The calculations are based on Eqs. (35)–(37) and on the first and the tenth sidebands of the restored power spectrum in Figs. 7(a) and 7(b) of Ref. 4. In (a) the integration boundaries are 25 Hz to 500 Hz, and in (b) and (c) these boundaries are 50 Hz to 500 Hz and 75 Hz to 50 Hz, respectively.

the results of Figs. 7(a) and 7(b) of Ref. 4. Figures 5(b) and 5(c) describe the same calculation of the normalized autocorrelations as in Fig. 5(a) but for different frequency ranges. In Fig. 5(b) the integration limits were from 50 Hz to 500 Hz, and in Fig. 5(c) the limits were 75 Hz to 500 Hz. It is clearly shown that the amplitude autocorrelation width (FWHM of the dashed curves) and shape, and the timing-jitter autocorrelation width and shape (FWHM of the solid curves), are of the same order, i.e., $\kappa_c \sim 1.2 \times 10^5$ to 1.6×10^5. This is equivalent to an autocorrelation time of the order of $t_c = k_c T$, i.e., of approximately 1.4 to 2 ms.

In the limit of our approximation to restore the data of the sidebands from Ref. 4, a clear negative autocorrelation is seen in Fig. 5 for pulses in the train separated by long time ($\sim 2k_c$). This indicates that the laser tends to produce both correlated and anticorrelated amplitude and timing-jitter fluctuations. A possible explanation for these results is a damped oscillation of the processes that are responsible for these fluctuations.

10. CONCLUSION

We have presented an analysis of the entire power spectrum of pulse trains in the presence of noise. The calculations were done with the assumption of stationary pulse-shape, amplitude, and timing-jitter fluctuations. Effects of correlations were studied as well.

We found that amplitude and timing-jitter convolution and their correlations appear as higher powers of their fluctuations in the power-spectrum sidebands. Their contributions to the power-spectrum integration is negligible whenever the fluctuations are small.

The effect of pulse-shape fluctuations was considered also. We found that these fluctuations have an influence on the side-bands similar to that of amplitude fluctuations. It was also found that the tail of the power-spectrum shape is changed as a result of these fluctuations. The spectrum envelope becomes broader and decays more slowly than without these fluctuations.

The nonstationary timing-jitter fluctuations of passively mode-locked lasers and their influence on the power spectrum was discussed briefly. The discrete lines and the ω^2 characteristic of the low-frequency power spectrum for stationary timing-jitter fluctuations in actively mode-locked lasers are not valid in this case. Instead, the sideband's peak values decay and its FWHM increase as the harmonic number increases.

The predictions are, generally, in agreement with experimental observations. An additional conclusion on the correlation times of amplitude and timing-jitter fluctuations could be achieved for the special case of relatively small amplitude fluctuations.

ACKNOWLEDGMENTS

This research was supported by the National Science Foundation and the Advanced Research Projects Agency.

REFERENCES

1. D. von der Linde, "Characterization of the noise in continuously operating mode-locked lasers," Appl. Phys. B **39,** 201–217 (1986).
2. M. L. Lambsdorff and J. Kuhl, "Low noise hybrid mode-locking of a femtosecond continuous wave dye laser with Gires–Tournois interferometers," J. Opt. Soc. Am. B **5,** 2311–2314 (1988).
3. M. J. W. Rodwell, D. M. Bloom, and K. J. Weingarten, "Subpicosecond laser timing stabilization," IEEE J. Quantum Electron. **25,** 817–827 (1989).
4. A. Finch, X. Zhu, P. N. Kean, and W. Sibbett, "Noise characterization of mode-locked color-center laser sources," IEEE J. Quantum Electron. **26,** 1115–1123 (1990).
5. P. A. Harten, S. G. Lee, J. P. Sokoloff, J. R. Salcedo, and N. Peyghambarian, "Noise in a dual dye jet hybridly mode-locked near infrared femtosecond laser," Opt. Commun. **91,** 465–473 (1992).
6. J. Son, J. V. Rudd, and J. F. Whitaker, "Noise characterization of a self-mode-locked Ti:sapphire laser," Opt. Lett. **17,** 733–735 (1992).
7. D. Henderson and A. G. Roddie, "A comparison of spectral and temporal techniques for the measurement of timing jitter and their application in a modelocked argon ion and dye laser system," Opt. Commun. **100,** 456–460 (1993).
8. A. Yariv, *Optical Electronics,* 4th ed. (Saunders, Philadelphia, Pa., 1991), p. 360.
9. H. A. Haus and A. Mecozzi, "Noise of mode-locked lasers," IEEE J. Quantum Electron. **29,** 983–996 (1993).
10. D. Eliyahu, R. A. Salvatore, and A. Yariv, "The effect of noise on the power spectrum of passively mode-locked lasers," submitted to J. Opt. Soc. Am. B.
11. I. G. Fuss, "An interpretation of the spectral measurement of optical pulse train noise," IEEE J. Quantum Electron. **30,** 2707–2710 (1994).